Vol 18 No 9, September 2009
1674-1056/2009/18(09)/3922-06

Chinese Physics B

© 2009 Chin. Phys. Soc.
and IOP Publishing Ltd

Synthesis and characterization of highly-ordered barium-strontium titanate nanotube arrays fabricated by sol–gel method*

Chen Yu(陈 煜)[a)b)], Chen Wei(程 伟)[a)], Guo Feng(郭 峰)[a)],
Li Mei-Ya(李美亚)[a)], Liu Wei(刘 威)[a)b)†], and Zhao Xing-Zhong(赵兴中)[a)b)‡]

[a)] *Department of Physics, Wuhan University, Wuhan* 430072, *China*

[b)] *Nanoscience and Nanotechnology Center, Wuhan University, Wuhan* 430072, *China*

(Received 3 March 2009; revised manuscript received 21 April 2009)

Highly uniformed barium-strontium titanate nanotube arrays were fabricated using a porous anodic aluminum oxide template from a barium-strontium titanate sol–gel solution. Electron microscope results showed that nanotubes with uniform length and diameter were obtained. The diameters and lengths of these nanotubes were dependent on the pore diameter and the thickness of the applied anodic aluminum oxide template. High resolution transmission electron microscopy and the selected-area electron diffraction pattern investigations demonstrated the perovskite structure and the polycrystalline of the fabricated barium-strontium titanate nanotubes. The characterization of the electrical and dielectric properties had also been made. Compared to thin film material, the intrinsic leakage current density is almost the same. Besides, at 30 °C, the dielectric constant and dielectric loss of the fabricated nanotube is 80 and 0.027 at 1 MHz respectively.

Keywords: nanotubes, barium-strontium titanate, sol–gel
PACC: 6146, 7280G, 8270

1. Introduction

During the last decade, nanomaterial, especially one dimensional nanostructures, has attracted a great deal of interest, mainly because of their unique properties relative to bulk materials. Various materials have been applied in the fabrication of nanowires and nanotubes, such as carbon,[1,2] $PbTiO_3$&$BaTiO_3$,[3,4] ZnO,[5] polymer,[6] and etc. Among all these materials, piezoelectric and ferroelectric nanostructures have drawn a great deal of attention mainly for their potential application in nanoscale piezoelectric transducers and actuators, ultrasonic devices, and memory devices.[7−11]

Perovskite (Ba, Sr) TiO_3 (BST) was a promising dielectric and ferroelectric material and has been widely researched for its application mainly for its properties of high dielectric constant, low leakage current density, low dielectric loss, and negligible aging and fatigue effects. These properties offer the possibility of BST for the next generation of integrated dynamic random access memories (DRAMs),[7] pyroelectric detectors,[12] hydrogen gas sensors,[13] tunable microwave devices[14] microelectromechanical systems (MEMS)[15] and even optical signal processing units.[16] BST bulk materials and thin film structures have already been widely researched. However, few reports had been published about its nanostructures.

Since the carbon nanotubes were successfully synthesized in 1991, numerous more advanced and efficient methods have been used to fabricate piezoelectric and ferroelectric nanostructure materials, such as Urban and coworkers who reported the synthesis of $BaTiO_3$ and $SrTiO_3$ nanorods with diameters ranging from 5 to 60 nm by a solution-phase decomposition of bimetallic alkoxide precursors in the presence of coordinating ligands.[17] Using such method, Hernandez *et al* first fabricated $BaTiO_3$ and $PbTiO_3$ nanotubes within 200 nm by using a sol–gel anodic alumina oxide (AAO) template synthesis method.[3] Compared with traditional methods to prepare one dimensional nanostructures such as nanolithography, e-beam lithography and x-ray lithography, the sol–

*Project is supported by the National Natural Science Foundation of China (Grant No 60244003).
†E-mail: wliu@whu.edu.cn
‡Corresponding author. E-mail: xzzhao@whu.edu.cn

gel template method is a more suitable alternative because of its advantages such as being less expensive, more efficient and more stable. As an important preparation method of nanostructure materials, template methods[18] play an important role in a variety of areas. Different kinds of template such as anodic porous alumina, polymer, and nanochannel glass templates have been widely investigated. Normally, anodized aluminum in an appropriate acid solution forms an anodic porous alumina template. The advantages of an AAO template over other templates such as Si are mainly its high density of pores, high uniformity of distribution and the controllable relation between the adjustable diameters of the pore with that of the nanotubes.[19]

In this paper, we report and fabricate highly-ordered BST nanotube arrays by utilizing the sol–gel method in combination with the AAO template. The characterization of its morphology, structure and electrical property has been made. Compared to bulk materials and thin films, the high uniformity, lower dimension and larger specific surface areas of such BST nanotubes offer a possible solution to the further improvement of the capacity of DRAM and the sensitivity of BST-based gas sensors.

2. Experimental

2.1. AAO membrane preparation

High-purity aluminum sheets (99.999%, 20 mm×10 mm) were used in this experiment. Prior to anodization, both sides of the aluminum surfaces were degreased, etched in alkaline solution, rinsed in distilled water, and electropolished to achieve a smooth surface. Then, we would immerse the samples in a concentrated acid or alkaline solution for several minutes to remove the oxide layer formed during the electropolishing process. After this deoxidation step, all samples were rinsed in distilled water and then transferred to a nitrogen environment. The resultant clean aluminum samples were anodized at a constant potential in 0.3 M oxalic acid ($C_2H_2O_4$) (40 V, 4 °C, Pt sheet as a counter electrode). The anode was then immersed in an aqueous solution of 0.6 M H_3PO_4 and 0.15 M H_2CrO_4 at 60 °C for 48 h to remove the alumina layer. Subsequently, the anode was anodized for 10 h in the same condition again and became an AAO template with highly ordered nanoporous arrays.

2.2. BST sol preparation

Barium acetate [$Ba(CH_3COO)_2$] and strontium acetate [$Sr(CH_3COO)_2$] were taken in the desired molar ratio and dissolved in heated glacial acetic acid. Ti isopropoxide [$Ti(OC_2H_4CH_3)_4$] was mixed with acetyl acetone (chelating agent) under a nitrogen atmosphere and then mixed with the acetate solutions drop by drop under constant stirring. 2-Methoxy-ethanol and formamide were added to the sol to adjust the viscosity of the sol. The transparent yellow sol was finally filtered using a Whatman glass-micro-fibre filter paper and stored as the stock solution.

2.3. BST nanotubes preparation

The alumina template membrane was dipped into the sol for the desired amount of time and removed, and the excess sol on the membrane surface was wiped off using a laboratory tissue, followed by drying under vacuum at 100 °C for 24 h. The membrane surface was carefully wiped again to remove salts crystallized on the surface and heated at 700 °C for 4 h in open air, resulting in the formation of arrays of BST nanotubes inside the pores of the AAO template.

2.4. Characterization

The morphologies of the BST nanotubes were characterized by a scanning electron microscope (SEM, Sirion FEG, FEI). Before the SEM observation, the BST/AAO sample was etched by 2M aqueous NaOH for 30 min. This sample was attached to a sample stub with adhesive tape without a thin layer of Au on the surface. Transmission electron microscopy (TEM) images and a selected-area electron diffraction (SAED) pattern were taken with a transmission electron microscope (TEM, JEM-2010, JEOL). High-resolution TEM (HRTEM) images were obtained on a JEOL-2010 HRTEM. Before TEM observation, the alumina template membrane was dissolved by using 3 M (1 M=1 mol/dm^3) NaOH, and then diluted with distilled water by three times. Droplets of solution containing BST nanotubes were dropped onto the copper grids. The voltage dependence of current density was measured using a ferroelectric test system Radiant Technologies RT3100 and the dielectric properties were measured by using an Agilent 4294A Precision Impedance Analyzer.

3. Result and discussion

The SEM images of BST nanotubes within the pores of the AAO template membranes are shown in Fig.1. Figure 1(a) shows BST nanotube arrays in a large area. It can be seen that the surface layer BST nanotubes tangle with each other and completely lose their original highly-ordered form within the template. The BST nanotubes under the surface layer are parallel to each other. The explanation for this chaotic arrangement of former ordered arrays is that the AAO template membranes in the surface layer, which functioned as the substrate to grew and confine the BST nanotubes, are dissolved completely. Thus, the upper part of the nanotubes broke down and fell onto the remained nanotubes.

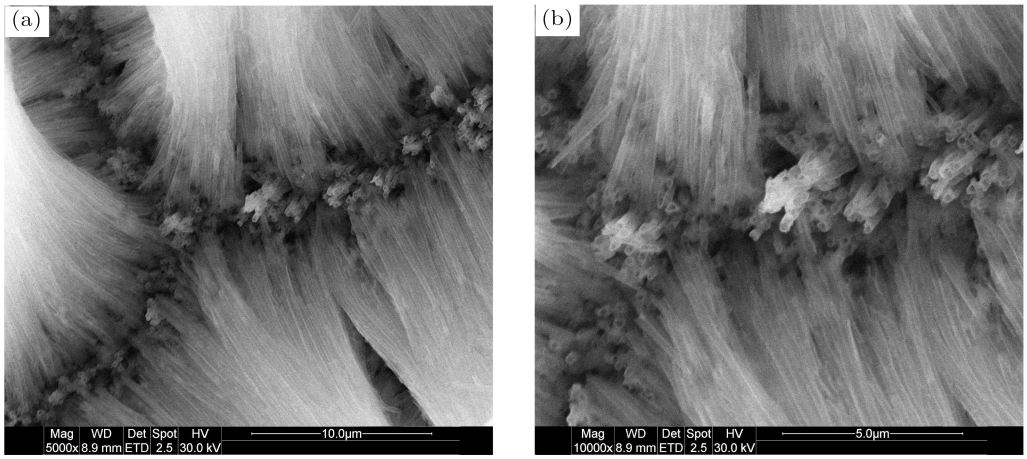


Fig.1. SEM images of BST nanotubes: (a) image of BST nanotube arrays in a large area; (b) enlarged magnification image of the top view.

A higher magnification image of Fig.1(a) is shown in Fig.1(b). It can be seen more clearly that nanotubes in the AAO template are parallel to each other, uniformly distributed in diameter and continue in the whole length without fracture. It is learly observed in this image that the diameter and the thickness of the wall of the nanotubes are generally 150 nm and 7–8 nm, respectively. Obviously, the pore-filling rate is extremely high, and the morphology of the BST arrays was controlled by the shape and density of the AAO pores.

According to different experimental conditions of the sol–gel method, the sol may contain various types of substances. In order to certify the existence of all the elements consisting of BST in the nanotubes, XPS patterns are shown in Fig.2. The XPS pattern of the BST nanotubes and the AAO composite is shown in Fig.2(a), where several characteristic peaks can be clearly observed and have been marked by the relative elements. The relationship between the specific element and the various characteristic peaks can be identified by detailed XPS patterns (Figs.2(b)–2(f)). We had measured the XPS patterns of the background element Al (Fig.2(b)) and patterns of those elements in the BST such as Ba (Fig.2(c)), O (Fig.2(d)), Sr (Fig.2(e)) and Ti(Fig.2(f)) before the examination of the BST/AAO composite. Comparing these peaks in Fig.2(a) with other XPS patterns, we can identify the existence and quantity of all the elements both in AAO and BST.

To further exam the morphology and crystal structure of a single nanotube, we had also made TEM and SAED measurements. Typical TEM images of the BST nanotubes formed within the AAO template are shown in Fig.3. The evidence for the formation of polycrystalline nanotubes of BST can be found in the high-resolution TEM (HRTEM) image and the selected-area electron diffraction (SAED) image in Fig.3. Figure 3(a) shows a single BST nanotube. This image clearly indicates that the diameter of a single BST nanotube is about 150 nm, which correspond exactly to that of the pore of the AAO templates. The thickness of the BST nanotubes can be found in the range of 7–8 nm from this image, which is also well matched to that formerly shown in

Fig.1(b).

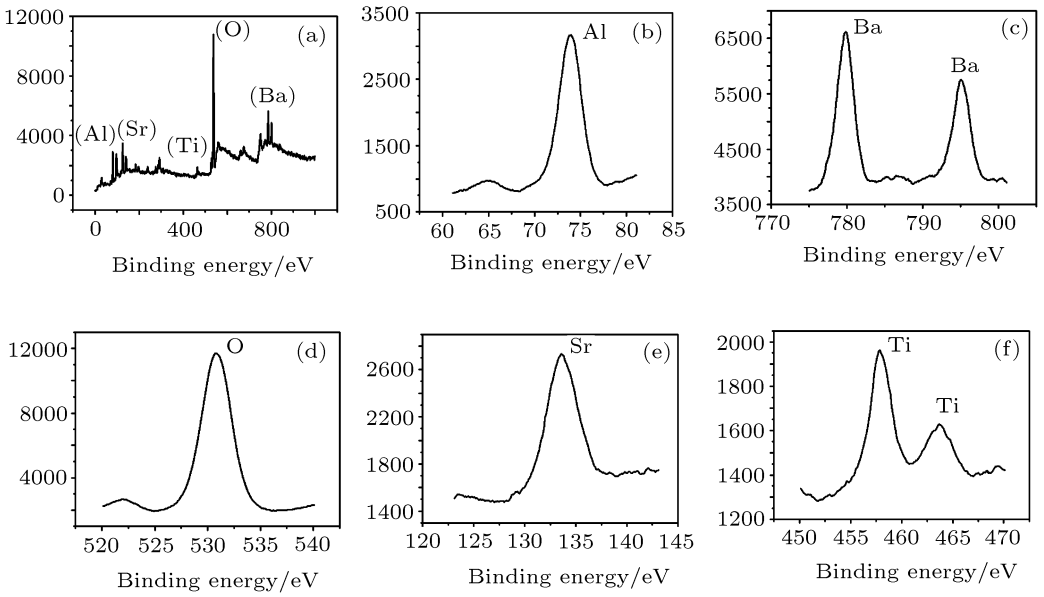


Fig.2. The XPS pattern of the BST/AAO composite: (a) BST/AAO composite; (b) Al; (c) Ba; (d) O; (e) Sr; (f) Ti.

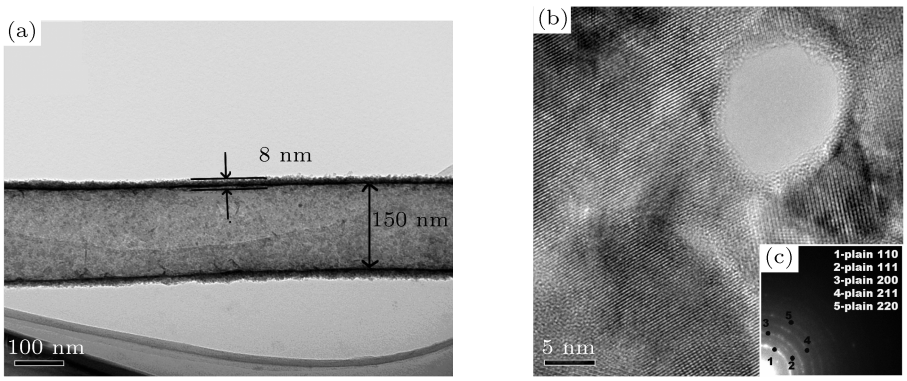


Fig.3. TEM images of BST nanotubes: (a)single BST nanotube, (b) HRTEM image of a single BST nanotube, (c) (inset of (b)) SAED pattern.

Figure 3(b) shows the HRTEM image of a single BST nanotube. We can observe the lattice fringes from this image and it reveals that the surfaces of the nanotubes are clean, very regular and without any sheath of the amorphous phase. The polycrystalline structure of the fabricated nanotubes is proved by several different directions of the lattice being observed. To further identify the structure of the nanotubes formed during the crystallization process in the AAO pores, a corresponding electron diffraction pattern was taken and shown in Fig.3(c) (inset in Fig.3(b)). Several bright diffraction rings are shown in this image, and it should be noted that the diffraction rings are continuous and actually consist of spots, which further indicate that the nanotubes are of a polycrystalline structure, but not monocrystalline. According to the electron-diffraction formula, the major diffraction rings correspond to the (110), (111), (200), (211) and (220) diffraction planes for BST with a cubic perovskite structure. So it can be concluded that the BST nanotube obtained in our experiment is polycrystalline and with a perovskite structure.

To measure the J–E curve of the BST nanotubes, we firstly mechanically polished both sides of the BST

nanotubes contained AAO template until the BST nanotubes emerged. Then, using the RF magnetron sputtering method, we deposited a layer of Au film with a thickness of nearly 100nm on both sides of the template, which functioned as cathode and anode. Different to bulk materials, such as the BST thin film, the contact area between the electrode and the nanotubes is less than 1 percent of the overall surface area of the Au film, and therefore, the measured J value was multiplied by 100 as the intrinsic value of J.[20] Figure 4 shows the J–E curve of the BST nanotubes. The leakage current property of the thin film of the BST had been widely researched by many groups and it is well known that the conducting mechanism of the metal–BST capacity is either the tunneling or the Schottky mechanism or a combination of both when the current conduction mechanism is electrode controlled.[21] From Fig.4, when the ow electric field was applied, a linear dependence relationship of J–V as the characteristic of ohmic behaviour can be clearly observed. When the applied E is approximately 2.4 kV/cm, a break of slope emerges, and then, when E exceeds 2.5 kV/cm the J–V characteristic behaved just as governed by the Schottky conduction mechanism. This phenomenon is consistent with that of the bulk materials.[22−25] The mechanism of the emergency of the slope break possibly is due to the change of the electron behaviour and the Schottky barrier height when the electric field is gradually increasing. When no bias electric field is applied, the deep acceptor states situated below the Fermi level were occupied by electrons. At some critical voltage

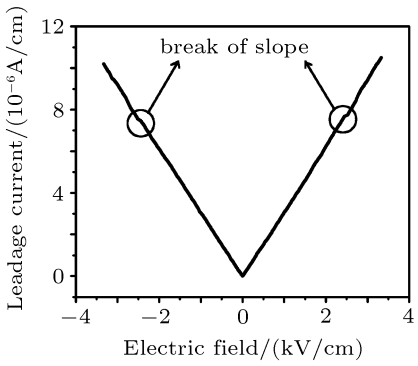


Fig.4. J–E curve of BST nanotubes.

(maybe just when E = 2.4 V/cm to our fabricated nanotubes) the 'quasi-Fermi' level cut off the acceptor states which lose their electrons, and would lead to a decrease of the height of the Schottky barrier between the metal–BST contact interface. And as the barrier is decreasing, the conduction mechanism would more easily change to Schottky behaviour. However, from Fig.4. we can observe that the nano size does not affect the leakage current characteristic of the BST material, the J–E characteristic of the BST nanotubes is generally consistent with those of the BST thin films as reported.[22]

Utilizing the same structure, we further measured the dielectric properties of such a BST nanotubes/AAO template composite. At room temperature 30 °C, we can observe from Fig.5 that the dielectric constant and dielectric loss of such a composite are about 16 and 0.027 respectively from 100 kHz to 1 MHz. Compared with the BST nanoparticles fabricated by the sol–gel method,[26] the dielectric constant of such a composite is somehow decreased. We consider that such a difference may come from the involvement of the AAO template as AAO possesses a low dielectric constant (2.25) due to its amorphous structure. Since this composite structure is a binary system which is composed of a nanotube with high dielectric constant (ε_2) dispersed in a matrix with low dielectric constant (ε_1), we could adopt the Jayasundere and Smith formula[27] to calculate the dielectric constant of the BST nanotubes. The expression is:

$$\varepsilon_{\text{eff}} = \{\varepsilon_1\nu_1 + \varepsilon_2\nu_2[3\varepsilon_1/(\varepsilon_2 + 2\varepsilon_1)] \times [1 + 3\nu_2(\varepsilon_2 - \varepsilon_1)/(\varepsilon_2 + 2\varepsilon_1)]\}/\{\nu_1 + [\nu_2(3\varepsilon_1)/(\varepsilon_2 + 2\varepsilon_1)] \times [1 + 3\nu_2(\varepsilon_2 - \varepsilon_1)/(\varepsilon_2 + 2\varepsilon_1)]\},$$

where ν_1, ν_2 is the volume fraction of the AAO template and BST nanotubes, respectively. From Fig.1(b), it is observed that the filling ratio of BST nanotubes is really high. Therefore, we assume the volume fraction of BST (ν_2) equals that of the AAO template (ν_2). The effective dielectric constant value is just the measured value which is 16 and ε_1 equals 2.25. Therefore, we could calculate that the estimated dielectric constant of the BST nanotubes is 80, which is smaller than that of the BST bulk material due to size effect. However, as clearly stated in Fig.5(b), the dielectric loss of fabricated BST nanotubes is almost the same as that of bulk materials[28] and nanopartical materials.[26] Thus, a conclusion that the good dielectric property of BST material could remain in such nanotubes structures has been drawn.

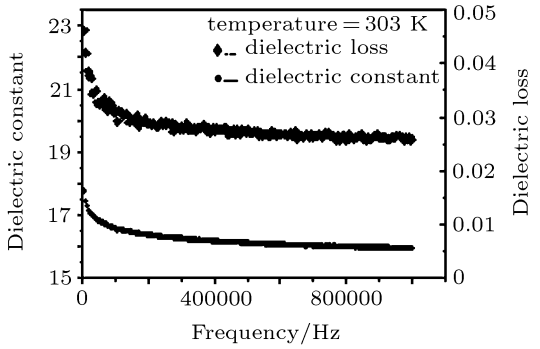


Fig.5. Dielectric properties of BST nanotubes with frequency.

The growth mechanism of BST nanotubes is suggested as below. Between the interface of the gel and the AAO template, as the generation of electroosmotic flow in capillary, the pore walls are negatively charged and the sol particles are positively charged causing the sol to adhere to the pore-cavity walls of the template. During the temperature ramping in the tube furnace, the sol within the AAO template changes into gel and further spontaneously burns liberating vapours such as H_2O, CO_2. High temperature sintering shrinks the gel and causes it to adhere to the template pores wall. Therefore, the length of the BST nanotubes is equal to the thickness of the applied template, and the outside diameter of these nanotubes is equivalent to the pore diameter of the AAO template.

4. Conclusion

BST nanotubes arrays were successfully fabricated by a sol–gel template process. Investigations of HRTEM and SAED patterns demonstrated that BST nanotubes have a perovskite structure of polycrystalline. Electron microscope results show that these BST nanotubes have a uniform length and diameter and form a highly ordered array, and which is determined by the pore diameter and the thickness of the applied AAO template. The lower dimension of such nanotubes has dramatically increased the specific surface area of the BST material with almost the same intrinsic leakage current density and dielectric properties. And such a one-dimensional nanostructure has provided us with the possibility to further improve the capability of BST-based devices.

References

[1] Baughman R H, Zakhidov A A and de Heer W A 2002 *Science* **297** 5582

[2] Wei J Q, Sun J L, Wu D H, Guo J H, Luo J B and Wang K L 2006 *Chin. Phys.* **15** 2731

[3] Bernadette A, Hernandez, Chang K S, Ellen R F and Peter K D 2002 *Chem. Mater.* **14** 480

[4] Morrison F D, Luo Y, Szaniafrak I, Nagarajan V, Wehrspohn R B, Steinhart R, Wendorff J H, Zarkharov N D, Mishina E D, Vorotilov K A, Sigov A S, Nakabayashi S, Alexe M, Ramesh R and Scott J F 2003 *Rev. Adv. Mater. Sci.* **4** 114

[5] Yang Y R, Yan X H, Guo Z H and Deng Y X 2008 *Chin. Phys.* B **17** 3433

[6] Steinhart M, Wendorff J H, Greiner A, Wehrspohn R B, Nielsch K, Schilling J, Choi J and Gosele U 2002 *Science* **296** 1997

[7] Hirata G A, López L L and Siqueiros J M 1999 *Superficiesy Vacio* **9** 147

[8] Chu M W, Szafraniak I, Scholz R, Harnagea C, Hesse D, Alexe M and Gosele U 2004 *Nat. Mater.* **3** 87

[9] Junquera J and Ghosez P 2003 *Nature* (London) **422** 6931

[10] Wang Y and Santiago-Aviles J J 2004 *Nanotechnology* **15** 32

[11] Luo Y, Szafraniak I, Zakharov N D, Nagarajan V, Steinhart M, Wehrspohn R B, Wendorff J H, Ramesh R and Alexe M 2003 *Appl. Phys. Lett.* **83** 440

[12] Zhang T J and Ni H 2002 *Sensors and Actuators* A **100** 252

[13] Zhu W, Tan OK, Yan Q and Oh J T 2000 *Sensors and Actuators* B **65** 366

[14] Xu J, Menesklou W G and Tiffee E I 2004 *J. Eur. Ceram. Soc.* **24** 1735

[15] Azuma M, Scott M C, Par De Araujo C A and Cuchiaro J D 1999 US Patent 08 **165** 082

[16] Roy D and Krupanidhi S B 1993 *Appl. Phys. Lett.* **62** 1056

[17] Urban J J, Yun W S, Gu Q and Park H 2002 *J. Am. Chem. Soc.* **124** 1186

[18] Schlottif F, Textor M, Gerrgi U and Roewer F 1999 *J. Mater. Sci. Lett.* **18** 599

[19] Gosele U, Li A P, Nielsch K, Muller F, Erfurth W and Wshrspohn R B 2000 *Extended Abstract 196th ECS Meeting* Toronto, Canada No. 158

[20] Liu W, Sun X H, Han H W, Li M Y and Zhao X Z 2006 *Appl. Phys. Lett.* **89** 163122

[21] Shin J C, Park J, Hwang C S and Kim H J 1999 *J. Appl. Phys.* **86** 506

[22] Gietz G W, Schumacher M and Waser R 1997 *J. Appl. Phys.* **82** 5

[23] Hu W C, Yang C R, Zhang W L and Liu G J 2007 *Ceramics International* **33** 1299

[24] Gao Y H, Sun J L, Ma J H, Meng X J and Chu J H 2008 *Appl. Phys.* A **91** 541

[25] Yang H, Chen B, Tao K, Qiu X G, Xu B and Zhao B R 2003 *Appl. Phys. Lett.* **83** 8

[26] Tomokazu T, Yoshio K, Takao M and Mikio K 2005 *Thin Solid Films* **485** 22

[27] Cho I S, Kang S K, Kim D W and Hong K S 2006 *J. Eur. Ceram. Soc.* **26** 2007

[28] Arya P R, Jha P and Ganguli A K 2003 *J. Mater. Chem.* **13** 415